J Electr Eng Technol.2018; 13(2): 829-837
http://doi.org/10.5370/JEET.2018.13.2.829

ISSN(Print) 1975-0102
ISSN(Online) 2093-7423

Indirect Detection of Rotor Position of Switched Reluctance Motor Based on Flux Linkage Analytic Model

Yongqin Zhou*, Bo Hu*, Hang Wang†, Ningzhi Jin* and Meilan Zhou*

Abstract – In this paper, a flux linkage model based on four magnetization curves fitting is proposed for three-phase 12/8 switched reluctance motor (SRM), with the analysis of the basic principle of flux detection method and function analysis method. In the model, the single value function mapping relationship between position angle and flux is established, which can achieve a direct estimation of rotor position. The realization scheme of SRM indirect position detection system is presented. It is proved by simulation and experiment that the proposed scheme is suitable for rotor position detection of SRM, and has high accuracy of position estimation.

Keywords: SRM, Flux linkage model, Rotor position, Indirect detection

1. Introduction

Switched reluctance motor (SRM) benefits from a relatively simple and rugged structure, so its application in hybrid electric vehicle has been a hot debate in the field of research [1]. SRM is a self synchronous motor with position closed loop, it is necessary to obtain the rotor information through the position sensor to guarantee its proper operation. The position sensor is used to detect the rotor commutation position in SRM, which provides the commutation information for the power converter. However, the existence of physical sensors bring a lot of defects and inconvenience for the application of SRM, such as increasing the complexity of the motor structure and reducing the operation reliability of the drive system [2]. So, methods which can determine the rotor position by using some electrical characteristics of SRM has became the focus of academic research. Under the condition of motor starting and low speed operation, the pulse excitation method is usually used, but the error becomes larger when the motor speed increases. The accurate estimation of the rotor position under the condition of operation is critical to the stable operation of SRM. Without accurate position information, an erroneous conduction phase will occur and the motor will not operate properly.

The flux linkage characteristic is a nonlinear function of the phase winding current and rotor position, reflecting the rotor position information [3]. The traditional flux linkage detection method is based on the relationship among flux, current and rotor position to establish three-dimensional data table [4-6]. Due to the single valued mapping relationship among the flux, current and position, the real-time position can be obtained by the interpolation of the look-up table. This method can realize continuous position estimation, but it is time-consuming to build three-dimensional data, the interpolation calculation is complex, and the accuracy of position detection depends on the precision degree of the three-dimensional table and also takes up a large memory space. Aiming at issues in the traditional flux detection method, a simplified flux linkage detection method is proposed in [7, 8]. It is based on the motor alternative single-phase conduction and current chopping control, namely, one phase is on when the other is off. Therefore, only by determining a phase commutation position, the three-dimensional data table of the flux linkage method can be simplified as a flux-current two-dimensional data table of the position alignment. The algorithm of this method is simple and fast, and its required hardware memory is small, which greatly takes full advantage of flux linkage method. But the commutation position is fixed, and the turn-on and turn-off angle cannot be optimized [9]. So the inaccurate estimation of turn-off position will result in the inaccurate estimation of turn-on angle. In order to obtain the continuous rotor position information under motor operating conditions, the mathematical expression is used to describe the nonlinear relationship among SRM's flux, current and position angle in [10-12], that is, the establishment of nonlinear analytical model of SRM. Because of the special double-salient structure and magnetic saturation characteristics of SRM, its electromagnetic characteristics exhibit high nonlinearity [13]. It is difficult to establish an accurate functional expression with theoretical deduction, and the establishment of an accurate and reliable analytical model is the most critical problem for the indirect detection of SRM position [14].

In this paper, based on the fundamental principle of flux

† Corresponding Author: Dept. of Electrical and Electronic Engineering, Harbin University of Science and Technology, Harbin, China. (zhouyongqin@hrbust.edu.cn)
* Dept. of Electrical and Electronic Engineering, Harbin University of Science and Technology, Harbin, China. (1217282685@qq.com, yanyu7856@foxmail.com, sharon0716@126.com, zhoumeilan001@163.com)
Received: June 22, 2017; Accepted: November 25, 2017

linkage method, an analytical model based on the four magnetization fitting curve is established on the basis of position detection scheme of function analytic model method. In this model, the piecewise function is used to describe the flux equation, and the single valued mapping function between the position angle and flux linkage is established. Since the model contains only one degree term of the rotor position angle, the rotor position angle can be reversely solved to get the rotor position information directly, in order to realize continuous estimation of rotor position. The simulation and experimental results show that the proposed scheme can well estimate the rotor position under the condition of SRM operation and has a high accuracy of position estimation.

2. The Principle of Flux Linkage Model Based Indirect Position Detection Method

The flux linkage is a periodic function of the rotor position angle, so the Fourier series analytical expression of the variable coefficient can be obtained by the special position alignment and nonalignment two magnetization curves. To retain more high-order terms of the Fourier series can increase the computational precision, but this increases the complexity of the model and the computational complexity of the control chip. Because of the harmonic components are much smaller than the fundamental component, the calculation model of 3rd harmonic component already has relative high engineering precision [15, 16]. The flux model can be expressed as a Fourier series expansion with the cubic term, shown in Eq. (1).

$$\begin{aligned}\psi(i,\theta) &= \sum_{n=0}^{3}\psi_n(i)\cos(nN_r\theta)\\ &= \psi_0(i)+\psi_1(i)\cos(N_r\theta)\\ &\quad +\psi_2(i)\cos(2N_r\theta)+\psi_3(i)\cos(3N_r\theta)\end{aligned} \tag{1}$$

Where $\psi(i,\theta)$ is the phase flux linkage; $\psi_n(i)$ is the flux linkage curve when under position $\theta = n$; i is the phase current.

According to the inherent symmetry of SRM structure,

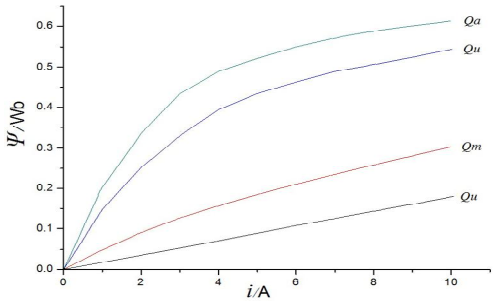

Fig.1. Static electromagnetic characteristic curves

the following four special angle positions are considered 0°, 7.5°, 15° and 22.5°, expressed as θ_u, θ_m, θ_n and θ_a respectively. It is required to determine the $\psi - i$ flux linkage curves at four special positions.

The flux linkage at four positions can be substituted into Eq. (1), and the relationships of the four magnetization curves can be resolved as Eq. (2).

$$\begin{aligned}\psi_u(i,\theta) &= \psi_0(i)+\psi_1(i)+\psi_2(i)+\psi_3(i)\\ \psi_m(i,\theta) &= \psi_0(i)+\frac{1}{2}\psi_1(i)-\frac{1}{2}\psi_2(i)-\psi_3(i)\\ \psi_n(i,\theta) &= \psi_0(i)-\frac{1}{2}\psi_1(i)-\frac{1}{2}\psi_2(i)+\psi_3(i)\\ \psi_a(i,\theta) &= \psi_0(i)-\psi_1(i)+\psi_2(i)-\psi_3(i)\end{aligned} \tag{2}$$

With the aid of Ansoft software, Four static electromagnetic characteristic curves of the prototype is obtained by finite element analysis, as shown in fig. 1, Under the θ_u position, the magnetization curve is basically linear, and the inductance of the motor at the θ_u position is L_u, which is suitable for linear fitting. The magnetization curve under θ_m, θ_n and θ_a positions is nonlinear and can be modeled as an exponential model.

$$\begin{aligned}\psi_{u0}(i,\theta) &= L_u i\\ \psi_m(i,\theta) &= L_{ms} i + a_m(1-e^{-b_m i})\\ \psi_n(i,\theta) &= L_{ns} i + a_n(1-e^{-b_n i})\\ \psi_a(i,\theta) &= L_{as} i + a_a(1-e^{-b_a i})\end{aligned} \tag{3}$$

L_{as} is incremental inductance in the saturation region, a and b are constants.

The unknown variables of the upper type are determined by the parameters of the motor itself, and the parameters of the prototype are as follows: L_u =0.017863H, L_{ms} = 0.021107H, a_m =0.095183, b_m =0.357589, L_{ns} =0.01466H, a_n =0.455811, b_n =0.398165, L_{as} =0.007567H, a_a = 0.530920, b_a =0.350209.

The complete analytic expression of the flux linkage can be obtained by substituting Eq. (2) and Eq. (3) into Eq. (1) :

$$\begin{aligned}\psi(i,\theta) &= \frac{1}{3}[\frac{1}{2}+\cos(N_r\theta)+\cos(2N_r\theta)+\frac{1}{2}\cos(3N_r\theta)]\times L_u i\\ &\quad +\frac{1}{3}[1+\cos(N_r\theta)-\cos(2N_r\theta)-\cos(3N_r\theta)]\\ &\quad \times[L_{ms} i + a_m(1-e^{-b_m i})]\\ &\quad +\frac{1}{3}[1-\cos(N_r\theta)-\cos(2N_r\theta)+\cos(3N_r\theta)]\\ &\quad \times[L_{ns} i + a_n(1-e^{-b_n i})]\\ &\quad +\frac{1}{3}[\frac{1}{2}-\cos(N_r\theta)+\cos(2N_r\theta)-\frac{1}{2}\cos(3N_r\theta)]\\ &\quad \times[L_{as} i + a_a(1-e^{-b_a i})]\end{aligned} \tag{4}$$

A simplified model is presented in [17], the SRM flux curves is approximated by the magnetization curves of two special positions of alignment and misalignment, but the calculation accuracy of the intermediate position magnetic flux linkage is relatively low. Therefore, this paper improves the accuracy by increasing the number of magnetization curves in the middle position.

Because the SRM magnetic circuit is nonlinear, the magnetic linkage is difficult to describe accurately by the analytic function of the current and the rotation angle, and the function fitting is generally required according to the modeling accuracy and the calculation speed. A fast modeling method based on function fitting can be used to describe the flux linkage model between any two flux curves [17]:

$$\psi(i,\theta)=\psi_{\theta_1}(i)+(\psi_{\theta_2}(i)-\psi_{\theta_1}(i))\cdot f(\theta) \tag{5}$$

where $\psi_{\theta 1}(i)$ is the flux curve corresponding to the position $\theta=\theta_1$, $\psi_{\theta 2}(i)$ is the flux curve corresponding to the position $\theta=\theta_2$, $f(\theta)$ is the rotor position function, only related to the rotor position angle, but to meet the following conditions:

$$\begin{cases} f(\theta=\theta_1)=0 \\ f(\theta=\theta_2)=1 \end{cases} \tag{6}$$

Regarding the following four special angular positions θ_u, θ_m, θ_n and θ_a corresponding to the four flux curves $\psi_u(i)$, $\psi_m(i)$, $\psi_n(i)$ and $\psi_a(i)$.

According to Eq. (5), the analytical model of flux linkage can be divided into three sections and described:

$$\begin{cases} \psi(i,\theta)=\psi_u(i)+\left[\psi_m(i)-\psi_u(i)\right]\bullet\left[m_0+m_1\cos\left(N_r\theta+\pi\right)\right], \\ \qquad\qquad\qquad\qquad\qquad\qquad\qquad\qquad\qquad\qquad \theta_u\le\theta<\theta_m \\ \psi(i,\theta)=\psi_m(i)+\left[\psi_n(i)-\psi_m(i)\right]\bullet\left[n_0+n_1\cos\left(N_r\theta+\pi\right)\right], \\ \qquad\qquad\qquad\qquad\qquad\qquad\qquad\qquad\qquad\qquad \theta_m\le\theta\le\theta_n \\ \psi(i,\theta)=\psi_m(i)+\left[\psi_n(i)-\psi_m(i)\right]\bullet\left[n_0+n_1\cos\left(N_r\theta+\pi\right)\right], \\ \qquad\qquad\qquad\qquad\qquad\qquad\qquad\qquad\qquad\qquad \theta_n<\theta\le\theta_a \end{cases} \tag{7}$$

By Eq. (6) can get $m_0=m_1=2$; $n_0=0.5$, $n_1=1$; $a_0=-1$, $a_1=2$. Table 1 is the comparisons of flux-linkage data at different rotor positions under the condition of current determination.

Table 1 shows that, the simplified model and the measured curves are quite different, especially in the middle position. The calculation accuracy of the model based on the four magnetization curves is obviously improved.

The rotor position angle can be obtained by the inverse deduction of model expression based on fitting four magnetization curves, so as to realize the position sensorless detection. By Eq. (7), we have:

Table 1. Comparisons of flux-linkage data at different rotor positions

Position angle (°)	Measured data	Simplified model		Four magnetization curve model	
	Flux linkage (Wb)	Calculation data	Error (%)	Calculation data	Error (%)
0	0.1245	0.1250	0.4	0.1250	0.4
2.5	0.1332	0.1385	3.9	0.1370	2.9
5	0.1615	0.1772	9.7	0.1717	6.3
7.5	0.2337	0.2366	1.2	0.2248	3.7
10	0.3128	0.3049	-2.5	0.3092	-1.1
12.5	0.4164	0.3824	-8.1	0.3990	-4.1
15	0.4931	0.4598	-7.3	0.4835	-1.9
17.5	0.5461	0.5191	-4.9	0.5302	-2.8
20	0.5687	0.5579	-1.8	0.5607	-1.3
22.5	0.5759	0.5713	-0.7	0.5713	-0.7

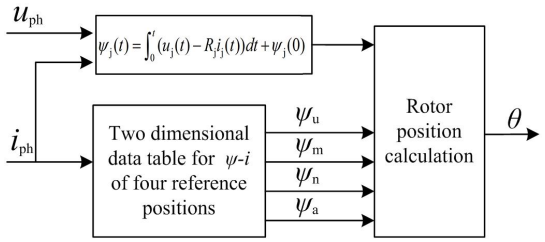

Fig. 2. Block diagram of position detection principle of the flux linkage model

$$\begin{cases} \theta=\dfrac{\pi}{N_r}-\dfrac{1}{N_r}\cos^{-1}\left(\dfrac{\psi(i,\theta)-\psi_u(i)}{\psi_m(i)-\psi_u(i)}\times\dfrac{1}{m_1}-\dfrac{m_0}{m_1}\right), \\ \qquad\qquad\qquad\qquad\qquad\qquad \psi_u(i)\le\psi(i,\theta)<\psi_m(i) \\ \theta=\dfrac{\pi}{N_r}-\dfrac{1}{N_r}\cos^{-1}\left(\dfrac{\psi(i,\theta)-\psi_m(i)}{\psi_n(i)-\psi_m(i)}\times\dfrac{1}{n_1}-\dfrac{n_0}{n_1}\right), \\ \qquad\qquad\qquad\qquad\qquad\qquad \psi_m(i)\le\psi(i,\theta)\le\psi_n(i) \\ \theta=\dfrac{\pi}{N_r}-\dfrac{1}{N_r}\cos^{-1}\left(\dfrac{\psi(i,\theta)-\psi_n(i)}{\psi_a(i)-\psi_n(i)}\times\dfrac{1}{a_1}-\dfrac{a_0}{a_1}\right), \\ \qquad\qquad\qquad\qquad\qquad\qquad \psi_n(i)<\psi(i,\theta)\le\psi_a(i) \end{cases} \tag{8}$$

According to Eq. (8), the rotor position angle can be calculated by the four flux linkage curves. The two-dimensional data table is established according to four flux linkage curves measured in advance. The flux linkage at four positions can be obtained according to the measured current through look-up table, which will be substituted into Eq. (8) to calculate the rotor angle. The block diagram of position detection principle is shown in Fig. 2.

3. System Implementation

The system composition of Sensorless SRM system based on flux linkage model is shown in Fig. 3, using the typical double closed loop control the outer speed loop with a PI regulator and the inner current loop with a hysteresis controller. The position sensorless detection

scheme is based on the flux linkage method and is adopted for position detection.

3.1 The calculation of rotor position angle

The voltage and current of the SRM excitation phase are sampled in real time, and the values of each sampling point are obtained by A/D conversion to calculate the corresponding real-time flux values. Meanwhile, according to the sampled real-time current and look-up table, the four reference position flux values are obtained, and then the rotor position angle can be calculated according to Eq. (8).

In the actual motor operation, due to the existence of interphase interference, measurement error, calculation error, modeling error etc., it will bring error to the position estimation. However, the estimated position angle in this method is calculated by the four reference positions, and the position estimation is calibrated at each reference position, so there will be no error accumulation. Furthermore, the calculation of the position angle changes continuously which can be corrected in real time if there is a singular point.

3.2 Calculation of turn-on angle and turn-off angle

The rotor position angle can be calculated continuously in real time, but it should be noted that to calculate the rotor position with Eq. (8) can only calculate the interval position angle [0°, 22.5°]. The equation can be used only when the excitation phase is within the interval, and when the excitation phase is turned off, the next phase must be followed.

Therefore, the turn-on angle of the next phase should not lag behind the turn-off angle of the excitation phase. Under this condition, the turn-on angle and turn-off angle can be set flexibly, so it is convenient to realize the optimal control of the turn-on and turn-off angles to achieve the high performance operation of the motor.

3.3 The calculation of speed

Because the four reference positions are fixed, the speed can be calculated by the time interval between any two reference positions:

$$\omega = \frac{\Delta\theta}{\Delta T} \tag{9}$$

In Eq. (9), ω is the angular speed of the motor, $\Delta\theta$ is the position angle distance between the two reference positions and ΔT is the time interval between the corresponding two reference positions. For the three-phase 12/8 pole motor selected in this paper and four reference positions, the $\Delta\theta = \frac{\pi}{24}$ can be calculated by selecting the minimal distance between the two adjacent positions, and the Eq. (9) is rewritten as:

$$\omega = \frac{\pi}{24 \cdot \Delta T} \tag{10}$$

4. Simulation analysis

4.1 Establishment of simulation model

Based on the idea of modular modeling, the simulation

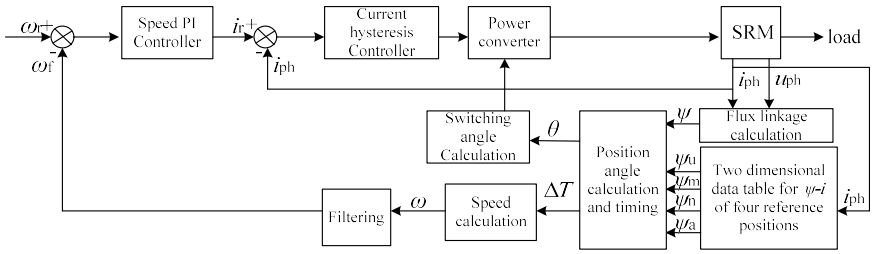

Fig. 3. Diagram of sensorless SRM system based on flux linkage model

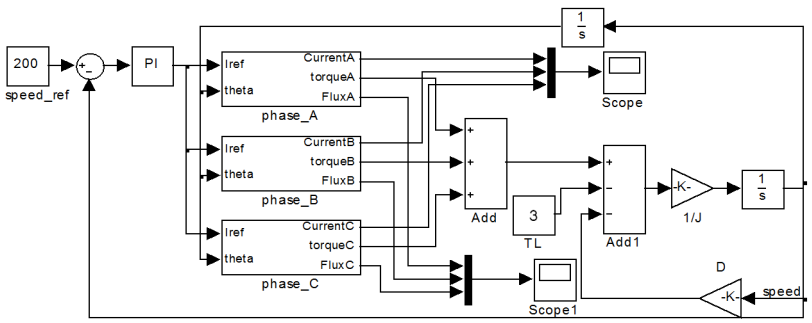

Fig. 4. Overall simulation model of the SRM system

model of the SRM sensorless control system is built up from the sub-modules with independent function. Each part of the system in Fig. 3 composes the simulation model using MATLAB Simulink. The overall simulation model of the SRM system is shown in Fig. 4.

4.2 Simulation of flux linkage model analysis

The prototype of this paper is a 3kW three-phase 12/8 pole SRM. The simulation parameters are set as: winding resistance is 2.47Ω, moment of inertia is 0.0082kg·m^2, friction coefficient is 0.008N·m·s, the turn-on angle is 0°, turn-off angle is 15°, the ratio of PI regulator is 18, the integral coefficient is 6, and the load torque is 3N·m.

Fig. 5 and Fig. 6 are the simulation waveforms of the estimated position and the actual position of the Phase A at different speeds. The actual position waveform is obtained directly from the angular velocity integral via the position sensor system, and the estimated position waveform is calculated using the Eq. (8). Fig. 5 is the simulation waveform of the actual position, the estimated position, the position error and the phase current of Phase A under 600r/min. In Figure a., the turn-on angle is 0°, and the turn-off angle is 15°; In Figure b, the turn-on angle is 0°, and the turn-off angle of 17°. Fig. 6 is the simulation waveform of the actual position, the estimated position, the position error and the phase current of Phase A under 3000r/min. In Figure a, the turn-on angle is 0°, and the turn-off angle is 15°; In Figure b, the turn-on angle is -1°, and the turn-off angle of 15°. In the simulation, the phase angle of each phase is estimated to be 0°-15°, and the position of the waveform is formed by the superposition of three phases in a periodical 45°position waveform.

It can be seen from the simulation waveform that the estimated position can approach the actual position at different speeds and different switching angles, with estimation error not beyond 0.3°, which has a high accuracy of position estimation. At low speed, the lag of the turn off angle has no influence on the position estimation, but the current amplitude is reduced, this is because the turn-on angle of each phase increases, while the load of the motor is constant, which leads to the smaller amplitude of the current command signal. Under high speed, the turn-on angle is leading, and the current rises more quickly. In the interval of [0°, 6°], the current is relatively large and stable, and the position estimation error is reduced. Meanwhile, the conduction angle of each phase increases and the current amplitude decreases. The

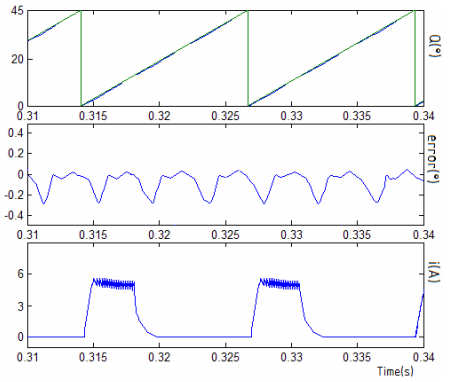

(a) turn-on angle is 0°, turn-off angle is 15°

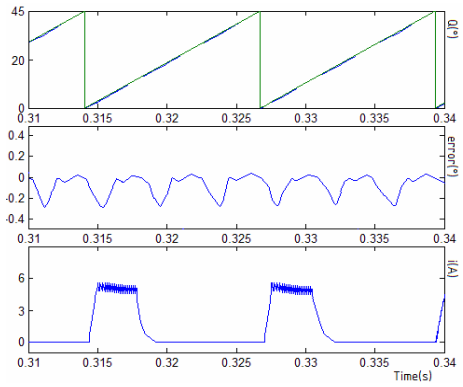

(b) turn-on angle is 0°, turn-off angle is 17°

Fig. 5. Simulation results at 600r/min

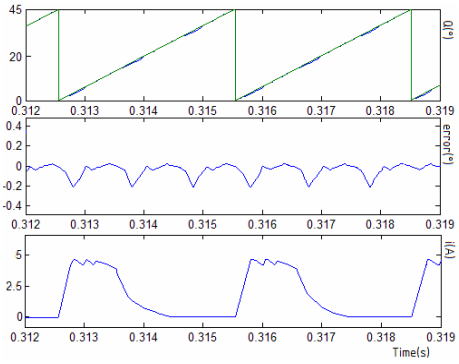

(a) turn-on angle is 0°, turn-off angle is 15°

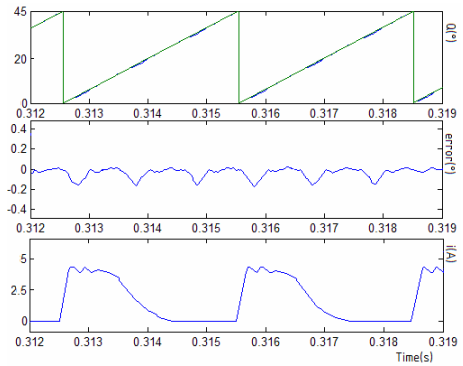

(b) turn-on angle is -1°, turn-off angle is 15°

Fig. 6. Simulation results at 3000r/min

simulation results are consistent with the theoretical analysis, which shows that the method can be used to detect the rotor position of SRM.

5. Experimental Analysis

SRM sensorless drive control system of the overall structure shown in Fig. 7. The experimental system consists of high power DC power supply, power converter, SRM, torque sensor, magnetic powder brake, power driver circuit, detection and protection circuit of various signals and DSP controller. The whole control system takes the TMS320F2812 chip as the core, and all the control algorithms, human-computer interaction and drive signal generation are controlled by the control chip. Due to DC bus voltage over 300V, the power conversion circuit uses three-phase asymmetrical half bridge circuit composed of IGBT, selection of photoelectric isolation drive, the modulation frequency is 10kHZ. The torque sensor is responsible for measuring the torque and speed of the motor. Magnetic powder brake is used as the load of motor. The control system also has the function of CAN communication, and the real-time data can be transmitted to the PC through the CAN interface, which is convenient for the analysis and research of the experimental results and the improvement of the control algorithm.

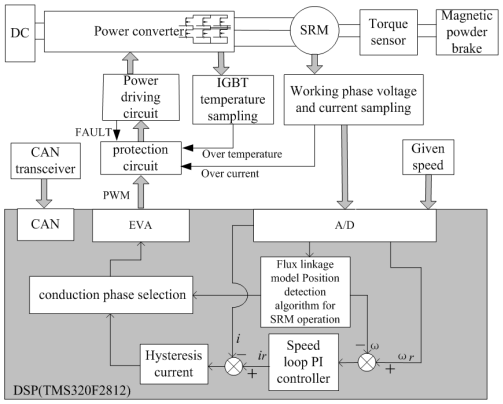

Fig.7. SRM sensorless drive control system

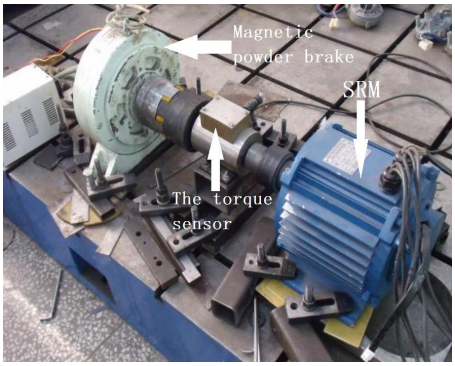

(a) SRM test bench

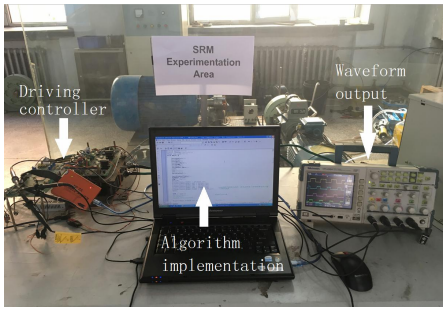

(b) SRM control platform

Fig. 8. Experimental platform of SRM drive system

5.1 Introduction of experimental platform

As shown in Fig. 8, experimental platform of SRM drive system, including test bench and control platform. The test bench is composed of motor, magnetic powder brake and torque sensor. Magnetic powder brake load motor, torque sensor can measure the torque and speed of SRM.

According to the experiment results, the effect of position detection method based on flux linkage model can be observed. The algorithm of flux linkage analysis model is compiled into the program module and embedded into DSP control program. The position waveform of the turn-on and turn-off of each phase winding is output through an I/O port, and the measured position data is output by the CAN bus. In this paper, the experimental system is equipped with three photoelectric coupling position sensors which can output the measured position information, and any phase position sensor can output the reference position signal interval of 45° angle position periodically. In this paper, the A phase reference position is taken as a reference. The reference position angle is calculated according to the real-time speed in every 45° position angle period. At the same time, the corresponding rotor position angle can be estimated by flux analysis method. The reference position angle and the estimated position angle are transmitted to the computer through the CAN bus for comparative analysis.

5.2 Experimental results analysis

By the experimental system of this paper, the photo-electric position sensor is started to run the motor, and the experimental conditions are identical with the simulation conditions. In order to be compared with the position sensor system, the turn-on angle is set to 0°, the turn-off angle is set to 15°, and the output of the I/O port is shown in Fig. 9. The Channel 1 shows the output position waveform of Phase A from the photoelectric sensor, and Channel 2, 3, 4 are the output position waveform of Phase A, B, C with the flux analysis method, respectively. The measured position data transfered from CAN bus are analyzed, so the Phase A reference position angle and the

corresponding estimation position angle data is obtained, which can be used to get the fitting curve and error curve between the estimated data and the measured data. A periodic waveform with the maximum angle error is shown in Fig. 10 and Fig. 11.

In Fig. 9, the output position waveform of the flux linkage model is almost consistent with the position waveform of the photoelectric sensor. The flux linkage model can stably estimate the turn-on angle and turn-off angle of each phase at different speeds.

As shown in Fig. 10 and Fig. 11, the estimated value fluctuates near the reference value. And the running error is larger when at low speed, this is because of the fluctuation of speed and current is relatively big when at low speed, which makes the integration operation produce a large cumulative error and the position estimation error is larger, too. After repeated test, the maximum error is 0.83°when at 600r/min. However, the error is small at high speed. That is because the speed and current are relatively stable at high speed, and the accumulated error of integral operation is small. After repeated test, the maximum error is 0.39°at 3000r/min.

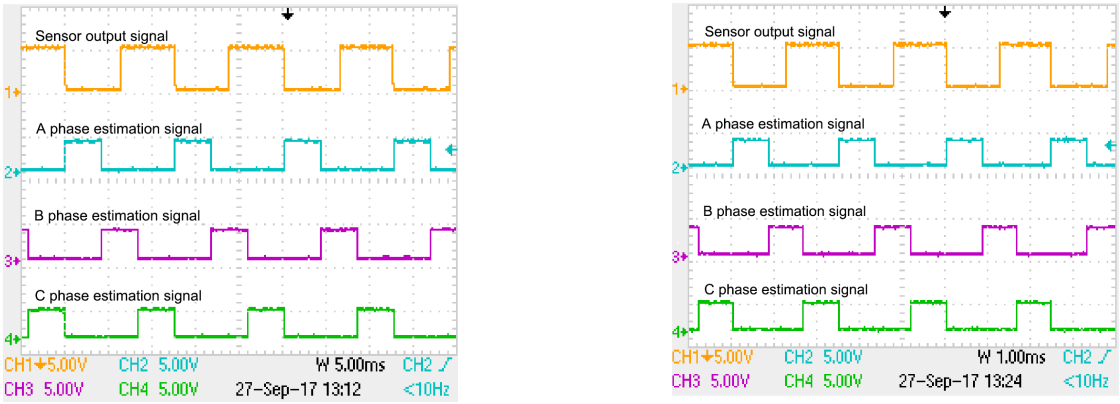

(a) 600r/min (b) 3000r/min

Fig. 9. The output waveform of flux linkage model

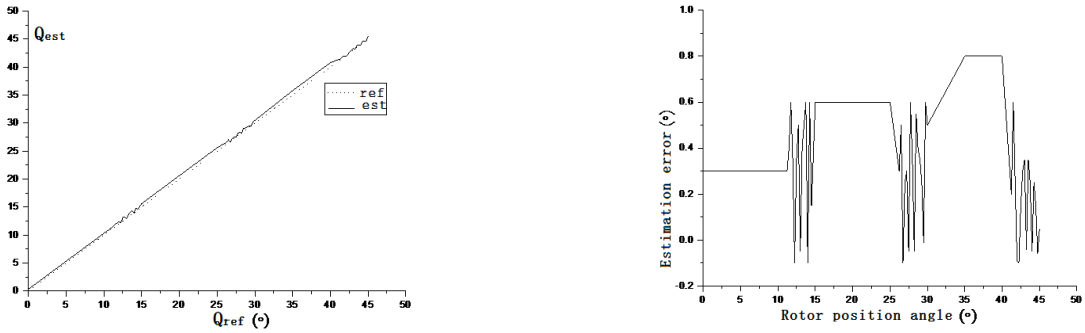

(a) Estimated curve (b) Error curve

Fig. 10. Analysis result of measured data at 600r/min

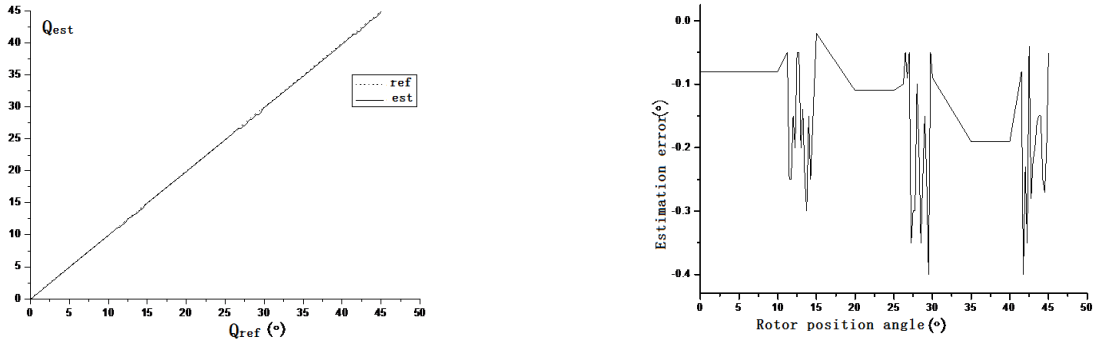

(a) Estimated curve (b) Error curve

Fig. 11. Analysis result of measured data at 3000r/min

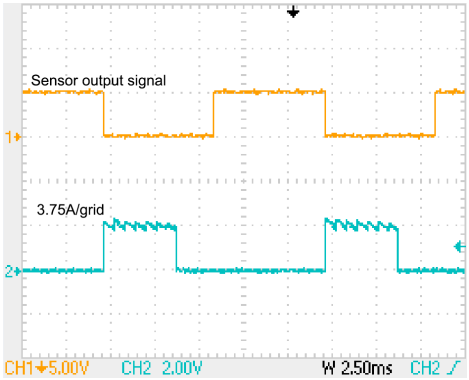

(a) 600r/min

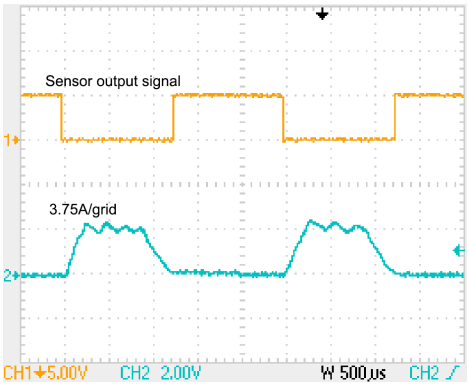

(b) 3000r/min

Fig. 12. Measured waveforms of rotor position and A phase current

Fig. 12 shows the measured rotor position and phase current waveform under the same simulation conditions. The channel 1 is the rotor position waveform generated by the photoelectric position sensor, and the channel 2 is the A phase winding current waveform. It can be seen that the simulation waveform is basically the same as the experimental waveform, which shows that the nonlinear modeling method proposed in this paper is correct and effective.

6. Conclusion

In this paper, on the analysis of the basic principle of flux linkage method, a SRM rotor position detection scheme based on flux analysis model is presented. The algorithm of the scheme is simple, with small hardware memory space and fast calculation speed. Moreover, the position estimation calibration at multiple reference positions can be adopted, which can eliminate the error accumulation and improve the accuracy of position estimation. Due to the continuous change of the position angle, if there is a singular point, it can be corrected on line, and thus the reliability of position estimation is improved. The simulation and experimental results show that the proposed scheme can estimate the rotor position angle of SRM very well.

Acknowledgements

This work is supported by Heilongjiang Natural Science Foundation (E2015063).

References

[1] Kiyota K., Kakishima T., Sugimoto H., et al., "Comparison of the test result and 3D-FEM analysis at the knee point of a 60kw SRM for a HEV," *IEEE Transactions on Magnetics*, vol. 49, pp. 2291-2294, 2013.

[2] U. Jakobsen, K. Lu, P.O. Rasmussen, et al., "Sensorless Control of Low-Cost Single-Phase Hybrid Switched Reluctance Motor Drive," *IEEE Transactions on Industry Applications*, vol. 51, pp. 2381-2387, 2015.

[3] Mao S.H., Dorrell D., Tsai M.C., "Fast analytical determination of aligned and unaligned flux linkage in switched reluctance motors based on a magnetic circuit model," *IEEE Transactions on Magnetics*, vol. 45, no. 7, pp. 2935-2942, 2009.

[4] Koblara T., Sorandaru C., Musuroi S.,et al., "A low voltage sensorless switched reluctance motor drive using flux linkage method," *International Conference on Optimization of Electrical and Electronic Equipment*, pp. 665-672, 2010.

[5] Chi H.P., Lin R.L., Chen J.F., "Simplified flux linkage model for switched reluctance motors," *IEEE Proceedings of Electrical Power Application*, vol. 152, pp. 557-583, 2005.

[6] Ding W., Liang D., "A fast analytical model for an integrated switched reluctance starter/generator," *IEEE Transactions on Energy Conversion*, vol. 25, pp. 948-956, 2010.

[7] D. Pinto, J. Pelletier, W. Peng, *et al.*, "Combined Signal-Injection and Flux-Linkage Approach for Sensorless Control of Switched Reluctance Machines," IEEE Vehicle Power and Propulsion Conference (VPPC), Hangzhou, pp. 1-6, 2016.

[8] Jia-Jun Wang, "A common sharing method for current and flux-linkage control of switched reluctance motor," ELECTR POW SYST RES 131 (2016) 19.

[9] Y. Zhang, C. Liu and L. Zhang, "Sensorless control of SRM based on improved simplified flux-linkage method," *2014 17th International Conference on Electrical Machines and Systems (ICEMS)*, Hangzhou, pp. 722-726, 2014.

[10] X. Zhang, Feng Wang and Xiaogen Shao, "Flux linkage characteristics on-line modeling of switched reluctance motor based on boundary constraints

RBF," Proceeding of the 11th World Congress on Intelligent Control and Automation, Shenyang, pp. 5942-5946, 2014.
[11] S. Song, L. Ge and M. Zhang, "Data-Reconstruction-Based Modeling of SRM with Few Flux-Linkage Samples From Torque-Balanced Measurement," *IEEE Transactions on Energy Conversion*, vol. 31, pp. 424-435, 2016.
[12] L.O. de Araujo Porto Henriques, L. G. Barbosa Rolim, W. Issamu Suemitsu, *et al*., "Development and experimental tests of a simple neurofuzzy learning sensorless approach for switched reluctance motors," *IEEE Trans. Power Electron*., vol. 26, pp. 3330-3344, 2011.
[13] F. Peng, J. Ye, A. Emadi, *et al*., "Position Sensorless Control of Switched Reluctance Motor Drives Based on Numerical Method," *IEEE Transactions on Industry Applications*, vol. 6, pp. 1-1, 2017.
[14] V. P. Vujičić and M. P. Ćalasan, "Simple Sensorless Control for High-Speed Operation of Switched Reluctance Generator," *IEEE Transactions on Energy Conversion*, vol. 31, pp. 1325-1335, 2016.
[15] Khalil A., Husain I., "A fourier series generalized geometry-based analytical model of switched reluctance machines," *IEEE Transactions on Industry Applications*, vol. 43, pp. 673-684, 2007.
[16] M.Stiebler, Ke Liu, "An analytical model of switched reluctance machines," *IEEE Transactions on Energy Conversion*, vol. 14, pp. 1100-1107, 1999.
[17] Hoang Le-Huy, P. Brunelle, "A Versatile Nonlinear Switched Reluctance Motor Model in Simulink using Realistic and Analytical Magnetization Characteristics," In Proceeding of Industrial Electronics Society, 2005.

Yongqin Zhou He received his PhD in Electrical Engineering from the Harbin University of Science and Technology. He is currently a Professor of Power Electronics and Power Drive, Harbin University of Science and Technology. His research interest includes the electric vehicle drive control and charging technology.

Bo Hu He received his Master's Degree from the Department of Electrical and Electronic Engineering in Harbin University of Science and Technology. His main research direction is the motor and motor drives.

Hang Wang He received his Master's Degree from the Department of Electrical and Electronic Engineering in Harbin University of Science and Technology. His main research direction is the Detection technology for sensorless position of switched reluctance motor.

Ningzhi Jin He received his PhD in Electrical Engineering from the Harbin University of Science and Technology. He is currently a Associate Professor of Power Electronics and Power Drive, Harbin University of Science and Technology. His research interest includes the motor drive technology for electric vehicles.

Meilan Zhou Professor, Ph.D., Master supervisor. Research directions: new energy vehicle electric drive control, automatic detection and intelligent control technology, PLC electrical control technology.